Proceedings of ICoEV 2015 International Conference on Engineering Vibration

Ljubljana, 7 - 10. September

CIP
National and University Library of Slovenia

621.8.034(082)(0.034.2)

INTERNATIONAL Conference on Engineering Vibration (2015 ; Ljubljana)
Book of abstracts of ICoEV 2015 [Electronic source] / International Conference on Engineering Vibration, Ljubljana, 7 - 10. September ; [editors Miha Boltežar, Janko Slavič, Marian Wiercigroch]. - EBook. - Ljubljana : Faculty for Mechanical Engineering, 2015

ISBN 978-961-6536-97-4 (pdf)
1. Boltežar, Miha
281005824

International Conference on Engineering Vibration
Ljubljana, Slovenia, 7-10 September 2015

Modelling of Heavy Vehicle Transmission Synchronizer using Constrained Lagrangian Formalism

Muhammad Irfan*, Viktor Berbyuk, Håkan Johansson

Department of Applied Mechanics
Chalmers University of Technology
SE - 412 96 Göteborg, Sweden
{irfan.muhammad, viktor.berbyuk, hakan.johansson}@chalmers.se

Keywords: Constrained Lagrangian Formalism, Generic Synchronizer, Synchronizer Performance, Sensitivity Analysis, Synchronization Time.

Abstract. *Robust and efficient synchronizers are keys elements to ensure good gear shift in heavy vehicles. In order to improve existing as well as develop new synchronizers, efficient simulation tools are needed.*

In this contribution, a mechanical system with 5 degrees of freedom modelling a generic synchronizer consisting of engaging sleeve, synchronizer ring and gearwheel are considered. Due to the design of the different components and their interactions the synchronizing process is described in terms of different steps or phases; presynchronization, main synchronization, blocker transition and engagement. The four main phases are further divided into sub-phases. To study the whole process in a unified manner, Constrained Lagrangian Formalism (CLF) turns out to be a suitable method in which the interactions between components (sleeve, synchronizer ring and gearwheel) are described by unilateral or/and bilateral constraints imposed on generalized coordinates of the system during different phases.

Using CLF a mathematical model of a generic synchronizer is developed and represented by the system of differential-algebraic equations. Kinematics and kinetics of the generic synchronizer are modelled for each sub-phase. The sleeve is considered as a master and the gearwheel is considered as a slave. The statement of the dynamics problem for a generic synchronizer is given and the numerical algorithm is implemented in Matlab for solving the differential-algebric equations resulting from CLF. The generic synchronizer computational model is adapted to available experimental setup and validated using obtained measurement data. Sensitivity of the synchronization time is studied varying the cone angle, coefficient of dry friction and sleeve force. Effect of driveline vibrations on synchronization performance is also studied.

1 INTRODUCTION

The demands for decreasing vehicle emissions, particularly for heavy vehicles, have led to higher demands on drive train components; by lower engine speed the gearbox must sustain higher torque, more torque vibrations and more frequent and faster shifts to keep engine running as close as possible to optimal speed. In order to design new synchronizers meeting these demands, simulation tools to study gearbox synchronizer performance are needed. The transmission system is a key element in motorized vehicles to transfer mechanical power from the engine to the wheels. It has great impact on the vehicle fuel consumption, power efficiency, noise and shift comfort. For manual transmission, synchronizer mechanisms were developed in the 1920s to allow smooth gear changing both for the durability of the transmission and the comfort for the users [1].

The gear synchronizer mechanism in its traditional design has the purpose that during released clutch, a new gearwheel is engaged by reducing the speed difference between outgoing shaft and the gearwheel to be engaged using a sleeve. This involves frictional contact between conical surfaces, and a design such that the sleeve is not engaged until the speed difference between sleeve and gearwheel is sufficiently small.

Lovas [2] explained the dynamics of the synchronizer and validate the numerical simulation results with the test bench measurements. Hoshino [3] simulated the synchronization mechanism by using ADAMS and studied the abnormal shift reaction force.

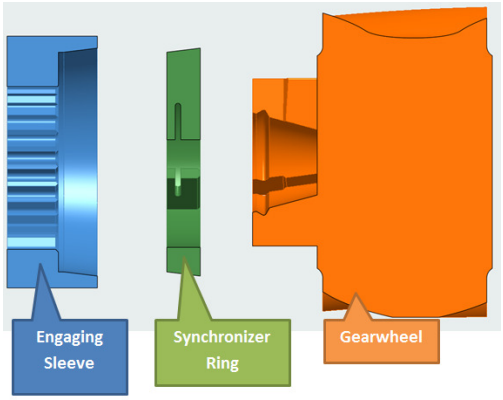

Figure 1: A common layout of a synchronizer.

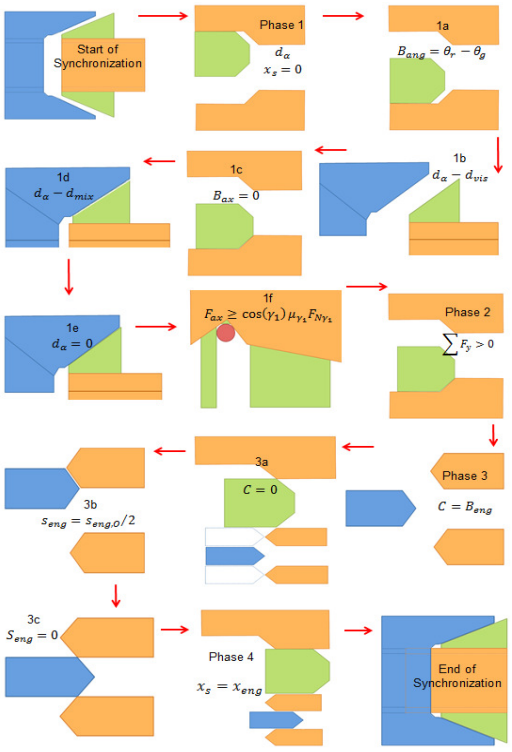

Figure 2: Division of synchronization in different phase events.

Kelly and Kent [4] developed a dynamic model to depict the entire selector system and correlated against the test data. Häggström and Nordlander developed a Matlab program for

the synchronization of transmission [5]. Transmission gear shifting improvement with respect to smooth, quick and energy efficient synchronizer performance is still one of the major concern areas for automotive industry and academia, see e.g [6-10].

Design optimization of synchronizer requires an efficient mathematical model. In this paper, a generic synchronizer is studied as a representative for common synchronizer designs used in manual and semi-automatic gearboxes. The considered synchronizer consists of an engaging sleeve, a synchronizer ring (also called blocker ring or baulk ring) and gearwheel. The engaging sleeve is attached to the gearbox output shaft (operated by gear selector) and the gearwheel is connected to the gearbox input shaft (clutch disengaged from motor). Constrained Lagrangian formalism is introduced in this paper to predict the dynamics of a generic synchronizer with emphasis on the different kind of interaction between bodies. Sensitivity of the synchronization time is analysed by varying the cone angle, coefficient of friction, rate of shift force, maximum allowable shift force and driveline vibrations with varying frequency and amplitude.

2 MODELLING OF A GENERIC SYNCHRONIZER MECHANISM

Here the equations of motion for a generic synchronizer are presented based on CLF. The kinematics of a generic synchronizer mechanism is determined from detailed description of the phases of the synchronization process.

2.1 Equations of motion

The generic synchronizer, as depicted in Figure 2 is considered as a multibody system (MBS) consisting of 3 rigid bodies

$$MBS = \{Engaging\ Sleeve, Synchronizer\ Ring, Gearwheel\} \tag{1}$$

The components are assembled on a shaft, on which the engaging sleeve and synchronizer ring may slide axially. The vector of generalized coordinates for the considered MBS is

$$\boldsymbol{q} = \left[x_s, \theta_s, x_r, \theta_r, \theta_g\right]^T \tag{2}$$

Here in θ_s, θ_r and θ_g are angular coordinates of the sleeve, ring and gearwheel, respectively; x_s and x_r are translational coordinates of the sleeve and ring, respectively. Following Lagrangian mechanics [12, 13], the Lagrangian L of the system is defined as

$$L = T(\boldsymbol{q}, \dot{\boldsymbol{q}}) - U(\boldsymbol{q}) \tag{3}$$

where $T(\boldsymbol{q}, \dot{\boldsymbol{q}})$ is a kinetic energy, $U(\boldsymbol{q})$ is a potential energy. Due to the design of synchronizer, the motion of the system is restricted by a set of holonomic kinematic constraints $\boldsymbol{\Phi}(\boldsymbol{q}, \boldsymbol{t}) = \boldsymbol{0}$. By introducing $\boldsymbol{\lambda}$ as the Lagrange multiplier vector, the motion of the system is described by a set of differential-algebraic equations (DAE)

$$\begin{cases} \left[\frac{d}{dt}\left(\frac{\partial L}{\partial \dot{\boldsymbol{q}}}\right)\right] - \left[\frac{\partial L}{\partial \boldsymbol{q}}\right] + \left[\frac{\partial \boldsymbol{\Phi}}{\partial \boldsymbol{q}}\right]^T \boldsymbol{\lambda} = \boldsymbol{Q}^A \\ \boldsymbol{\Phi}(\boldsymbol{q}, \boldsymbol{t}) = \boldsymbol{0} \end{cases} \tag{4}$$

where $\boldsymbol{Q}^A$ is a vector of generalized forces due to non-conservative applied loads. The vector of non-conservative forces $\boldsymbol{Q}^A$ is further divided into $\boldsymbol{Q}^A = \boldsymbol{Q}^A_{app} + \boldsymbol{Q}^A_{fric}$ where $\boldsymbol{Q}^A_{fric}$ are forces arising due to friction between bodies and other losses and $\boldsymbol{Q}^A_{app}$ are applied forces arising from external stimuli. For the generic synchronizer under consideration, Eq. (4) is written as follows

$$\begin{cases} \begin{bmatrix} m_s & 0 & 0 & 0 & 0 \\ 0 & I_s & 0 & 0 & 0 \\ 0 & 0 & m_r & 0 & 0 \\ 0 & 0 & 0 & I_r & 0 \\ 0 & 0 & 0 & 0 & I_g \end{bmatrix} \begin{bmatrix} \ddot{x}_s \\ \ddot{\theta}_s \\ \ddot{x}_r \\ \ddot{\theta}_r \\ \ddot{\theta}_g \end{bmatrix} + \left[\frac{\partial \boldsymbol{\Phi}}{\partial \boldsymbol{q}}\right]^T \boldsymbol{\lambda} = \begin{bmatrix} F_s \\ 0 \\ 0 \\ 0 \\ 0 \end{bmatrix}^{app} - \begin{bmatrix} F_{sf} \\ M_{sf} \\ F_{rf} \\ M_{rf} \\ M_{gf} \end{bmatrix}^{fric} + \begin{bmatrix} C_{s\alpha}\, sign(\dot{x}_s) \\ C_s \dot{\theta}_s \\ C_{r\beta}\, sign(\dot{x}_r) \\ C_r\, \dot{\theta}_r \\ C_g\, \dot{\theta}_g \end{bmatrix}^{oil,losses} \\ \boldsymbol{\Phi} = \begin{bmatrix} \boldsymbol{\Phi}^{imposed} \\ \boldsymbol{\Phi}^{internal} \end{bmatrix} = \mathbf{0} \text{ where } \boldsymbol{\Phi}(\boldsymbol{q}, \boldsymbol{t})^{imposed} = \theta_s - \omega_s t \end{cases} \quad (5)$$

where F_s is the applied shift force and $F_{rf} = -F_{sf}$, $M_{rf} = M_{gf} = -M_{sf}$. The set of internal constraints and parameters values is detailed in Table 1.

2.2 Different phases of a synchronization process

In the process of synchronization of the gear shift, different parts interact with each other to ensure the engagement or disengagement without clashing of the teeth. In this study, the division of the synchronization is not only based on relative position of the parts but also on interaction of the parts to capture the forces arising during synchronization. Each phase will be described in detail below. Pertinent constraints are given in Table 1 and the different events are shown in Figure 2.

Phase 1-Presynchronization. The phase 1 has the purpose of indexing. It starts from neutral position and ends where the axial force overcomes the axial resistance of the detent after contact of the synchronizer ring's chamfer with the gear's chamfer.

Here the phase 1 is further divided into different sub-phases based on the relative movement of the sleeve, the synchronizer ring and the gearwheel and varying oil film thickness between cone surfaces leading to identify the viscous, mixed and solid friction states.

Phase 1a-Angular indexing of the ring. Splines of the ring and the gear will be in contact at top as shown in Figure 2. At start of the phase 1a torque transfers from the sleeve to the ring through oil film and the ring will get angular rotation. After a while splines of the ring and the gear will come in contact at bottom at end of the phase 1a. The axial clearance between the cones is d_α.

Phase 1b-Free flight. The sleeve continues to move axially and oil film thickness decreases. The phase 1b ends when viscous friction must be taken into account at particular oil film thickness.

Phase 1c-Axial indexing of the ring. Chamfers of the gearwheel and the ring are at an axial clearance B_{ax}. The sleeve and the ring with oil film thickness d_{vis} move axially together until the chamfers come in contact.

Phase 1d-Viscous friction. The phase 1d is viscous friction phase when the oil between cones is squeezed out until the conditions between cones are shifted to mixed friction.

Phase 1e-Mixed friction. Axial clearance between the cones at start of the event is $d_\alpha - d_{vis}$ and at end is $d_\alpha - d_{mix}$. The phase 1e corresponds to mixed friction condition between cones.

Phase 1f-Force buildup. In this phase the amount of shift force further exceeds the detent axial resistance offered by the spring stiffness. The sub-phase will end when the condition will meet $\sum F_{ax} = F_s \geq \cos(\gamma_1)\, \mu_{\gamma_1} F_{N\gamma_1}$ where γ_1 is the detent angle and $F_{N\gamma_1}$ is the normal force at contact between detent and spring.

Phase 2-Main synchronization. Here the shift force increases while there is no axial movement of the sleeve and the transferred torque from cone friction will cause the rotation speed of the slave system (gearwheel) to adjust to the master system (sleeve). The phase 2 will end when the sleeve again starts to move axially and blocking torque at chamfers contact increases the cone torque or when the condition meets $\sum F_y > 0$.

Phase 3-Blocker transition. During the phase 3 the speed difference further decreases and reaches zero. The shift force is also needed to move the sleeve and the ring axially but the shift force will drop down from start of the phase 3. A detailed description for feasible and unfeasible synchronization is given in [11]. "Double bump" due to squeezing of oil between chamfers, turning of gear and cone sticking occurs during this phase.

Phase 3a-synchronized. Clearance c between the engaging teeth decreases to zero and the engaging teeth chamfers come in contact with a zero rpm difference. $B_{eng} = c = 0$ where B_{eng} is chamfers axial length.

Phase 3b-synchronized. Before the phase 3b the engaging teeth chamfers are at clearance S_{eng} and after the phase the chamfers come in full contact as shown in Figure 2. Relative rotational speed of the gear will be determined from the axial speed of the sleeve $\omega_g = \frac{v_s}{r_\beta} \tan\beta$ where r_β is mean radius at chamfers contact and β is angle of chamfers.

Phase 3c-synchronized. The phase 3c ends when the engaging teeth chamfers come out of contact and $S_{eng} = 0$.

Phase 4-Engagement. This is last phase of the synchronization where the engaging teeth get the engagement for transmission of the torque. The shift force is just needed to translate the sleeve and the ring for engagement of the teeth. The sleeve covered displacement x_{eng}.

Phase	Constraint: $\boldsymbol{\Phi(q,t)^{internal}}$	Phase	Constraint: $\boldsymbol{\Phi(q,t)^{internal}}$
1a	$[x_r]$=0	2	$\begin{bmatrix} x_r - d_\alpha \\ \theta_r - \theta_g - B_{ang} \end{bmatrix}$=**0**
1b	$\begin{bmatrix} x_r \\ \theta_r - \theta_g - B_{ang} \end{bmatrix}$=**0**	3a	$\begin{bmatrix} x_s - x_r - d_\alpha \\ \theta_r - \theta_g - B_{ang} - \frac{x_r - B_{ax}}{r_\beta}\tan\beta \end{bmatrix}$=**0**
1c	$\begin{bmatrix} x_s - x_r - d_{vis} \\ \theta_r - \theta_g - B_{ang} \end{bmatrix}$=**0**	3b	$\begin{bmatrix} x_s - x_r - d_\alpha \\ \theta_r - \theta_g - B_{ang} - \frac{x_r - B_{ax}}{r_\beta}\tan\beta \end{bmatrix}$=**0**
1d	$\begin{bmatrix} x_s - x_r - d_{mix} \\ \theta_r - \theta_g - B_{ang} \end{bmatrix}$=**0**	3c	$\begin{bmatrix} x_s - x_r - d_\alpha \\ \theta_r - \theta_g - B_{ang} - \frac{x_r - B_{ax}}{r_\beta}\tan\beta \end{bmatrix}$=**0**
1e	$\begin{bmatrix} x_s - x_r - d_\alpha \\ \theta_r - \theta_g - B_{ang} \end{bmatrix}$=**0**	4	$\begin{bmatrix} x_s - x_r - d_\alpha \\ \theta_r - \theta_s + \theta_{r\_s} \\ \theta_r - \theta_g - B_{ang} + \theta_{g\_s} \end{bmatrix}$=**0**
1f	$\begin{bmatrix} x_s - x_r - d_\alpha \\ \theta_r - \theta_g - B_{ang} \end{bmatrix}$=**0**		

Table 1: Internal constraints during subphases of the synchronization.

Here in Table 1 θ_{r_s} is difference in angular displacement between the ring and the gearwheel and θ_{g_s} is difference in angular displacement between the sleeve and the gearwheel before the phase 4.

3 DYNAMICS OF A GENERIC SYNCHRONIZER MECHANISM

In this section, the statement of the dynamics problem for a generic synchronizer mechanism is given and simulation results for a main gear downshift case are shown. The sleeve is taken as master and the gearwheel as slave. Downshift implies that the sleeve has high constant (prescribed) rotational speed and gearwheel has initially a lower speed that is to be synchronized to the sleeve speed. Sensitivity analysis of the synchronization time with respect to cone angle and coefficient of friction is also presented.

3.1 Problem formulation and synchronizer performance diagram

Problem A. Given the axial force acting on the sleeve, $F_s(t)$ (shift force), and the sleeve rotational speed $\dot{\theta}_s(t)$ during the synchronization process, i.e. for all $t \in [0, t_s]$.

It is required to determine motion of the sleeve, the ring and the gearwheel as well as contact forces between the sleeve and the ring and between the gearwheel and the ring that all together satisfy the differential-algebraic equations of motion, Eqs. (5), the initial conditions

$$\begin{cases} x_s(0) = x_s^0 & \dot{x}_s(0) = 0 & x_r(0) = x_r^0 & \dot{x}_r(0) = 0 \\ \theta_s(0) = \theta_s^0 & \dot{\theta}_s(0) = \dot{\theta}_s^0 & \theta_r(0) = \theta_r^0 & \dot{\theta}_r(0) = \dot{\theta}_r^0 \end{cases} \quad \theta_g(0) = \theta_g^0 \quad \dot{\theta}_g(0) = \dot{\theta}_g^0 \tag{6}$$

and the final conditions

$$\begin{cases} x_s(t_s) = x_s^s & \dot{x}_s(t_s) = \dot{x}_s^s & x_r(t_s) = x_r^s & \dot{x}_r(t_s) = \dot{x}_r^s \\ \theta_s(t_s) = \theta_s^s & \dot{\theta}_s(t_s) = \dot{\theta}_s^s & \theta_r(t_s) = \theta_r^s & \dot{\theta}_r(t_s) = \dot{\theta}_r^s \end{cases} \quad \theta_g(t_s) = \theta_g^s \quad \dot{\theta}_g(t_s) = \dot{\theta}_g^s$$
$$\dot{\theta}_s(t_s) = \dot{\theta}_r(t_s) = \dot{\theta}_g(t_s) = \omega \tag{7}$$

Here in Eqs. (6) and (7): x_s^0, θ_s^0, θ_r^0, $\dot{\theta}_s^0$, $\dot{\theta}_r^0$, θ_g^0 and $\dot{\theta}_g^0$ are arbitrary prescribed parameters; the synchronization time t_s to be determined; x_s^s, $\dot{x}_s^s$, x_r^s, $\dot{x}_r^s$, θ_r^s and θ_g^s are determined at the end of the synchronization process. The Eqs. (7) expresses the synchronization conditions.

To solve the Problem A, a computational model of the dynamics of the synchronizer mechanism in question was developed in MATLAB. The core of the computational model is implementation of predictor-corrector type algorithm [12, 13] to solve the system of DAE Eqs. (5) with initial and boundary conditions given by Eqs. (6) and (7).

3.2 Numerical solution of Problem A

For simulation of the dynamics of the generic synchronizer mechanism the particular input data is used as shown in Table 2.

$$F_s(t) = \begin{cases} \dot{F}_s t & t_0 \le t_{F_{s,max}} \\ F_{s,max} & t_{F_{s,max}} \le t_{phase,2} \\ 300 + \dot{F}_{s,3} t & t_{phase,2} \le t_{phase,3a} \\ F_{bumb} + \dot{F}_{s,3} t & t_{phase,3a} \le t_{end} \end{cases}$$

where $\dot{F}_{s,3}$ is decreasing force rate and F_{bumb} is double bump force.

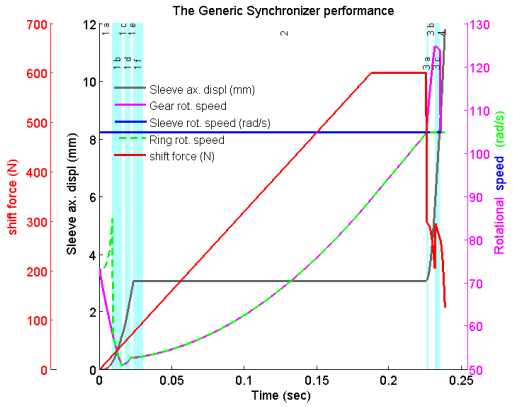

Figure 3: Synchronizer performance diagram.

As an example of the solution of the Problem A the axial position of sleeve and synchronizer ring, as well as sleeve force and rotational speeds of sleeve, ring and gearwheel

are collected in the diagram as shown in Figure 3, where also duration of sub-phases are shown.

As it follows from Figure 2 when the sleeve moves during the phase 1a and phase 1b the rotational speed of gearwheel and ring will decrease because of the oil splash losses. During the phase 1c the oil thickness between the cones is also not sufficient to transfer the torque from the sleeve to the gear. From the phase 1d to start of the phase 2 the gear almost retain its speed but the shift force increases to break the oil film thickness between the cones. From the phase 2 increment in the shift force is the main cause to increase gear speed while during phase 3, speed difference is because of turning of the gearwheel by the sleeve indirectly.

Variable	Name	Variable	Name
$m_s = 1.5$ kg	Sleeve mass	$m_r = 0.5$ kg	Ring mass
$m_{spr} = 0.2$ kg	Spring ring mass	$I_s = 0.01$ kgm^2	Sleeve moment of inertia
$I_r = 0.004$ kgm^2	Ring moment of inertia	$I_g = 0.2$ kgm^2	Gear moment of inertia
$r_\alpha = 0.1$ m	Cones mean radius	$r_\beta = 0.07$ m	Chamfers mean radius
$r_{spr} = 0.04$ m	Spring mean radius	$F_{spr} = 50$ N	Spring force
$b = 5$ mm	Cones contact length	$d_\alpha = 2$ mm	Cones Initial clearance
$d_{vis} = 1$ mm	Viscous friction clearance	$h_{min} = 0.1$ mm	Mixed friction clearance
$T_{oil} = 90^o$ C	Temperature at start	$\Delta T_{oil} = 20^o$ C	Temperature change
$\alpha = 7^o$	Cone angle	$B_{ang} = 5^o$	Angular clearance
$\beta = 60^o$	Chamfer angle	$\gamma = 5^o$	Detent angle
$\rho = 15$ mm^2/s	Oil viscosity [2]	$\mu_\alpha = 0.17$	Cones friction coefficient
$C_g = 5$	Gear oil splash losses	$C_s = 1$	Sleeve oil splash losses
$C_r = 0.003$	Ring sliding friction	$C_{s\alpha} = 0.02$	Sleeve sliding friction
$\omega_{s_o} = 1000$ rpm	Sleeve rotational speed	$\omega_{g_o} = 700$ rpm	Initial gear rotational speed
$\mu_{spr} = 0.12$	Spring friction coefficient	$\mu_\beta = 0.09$	Chamfers friction coefficient
$C_{r\alpha} = 0.002$	Ring sliding friction	$T_c = \lambda_{cons}\,\mu_\alpha F_s$	Cone Torque [2]
$F_{sf} = 16\pi\rho\dot{x}_s \sin(\alpha)\ r_c \left(\frac{b}{h}\right)^3$		Axial force transferred during viscous friction [2]	
$M_{sf} = 4\pi\rho\dot{x}_s r_c^3\ \omega_s \frac{b}{h}\left(1 - \frac{\omega_g}{\omega_s}\right)$		Torque transfer in viscous friction [2]	
$F_{s,max}$		Maximum acceptable applied shift force	

Table 2: Input parameters for the generic synchronization process.

4 SENSITIVITY ANALYSIS

A sensitivity analysis is done in order to see how cone angle, coefficient of friction and how the sleeve force affect the predicted synchronization time. In Figure 4 the synchronization time decreases with decreasing cone angle α and with increasing coefficient of friction μ. In Figure 5 the synchronization time decreases with increasing $F_{s,max}$ and $\dot{F}_s$. For higher values of the $F_{s,max}$ and $\dot{F}_s$ the synchronization time decreases rapidly than at lower values.

One problem of synchronizer design is its sensitivity to driveline vibrations. Here, the prescribed output shaft speed is modelled as $\omega_s = A\sin(2\pi f t + \vartheta)$ with frequency f and amplitude A. The sensitivity of synchronization time with respect to amplitude and frequency is shown in Figure 6 and 7. Since the phase shift is a random parameter $\vartheta \in [0, 2\pi]$, the mean synchronization time for 200 different values of ϑ is depicted.

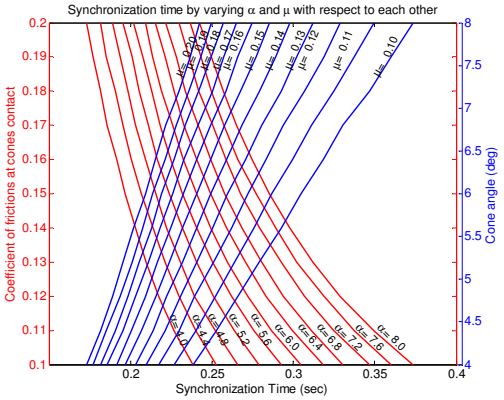

Figure 4: Synchronization time at varying cone angle α and coefficient of friction μ.

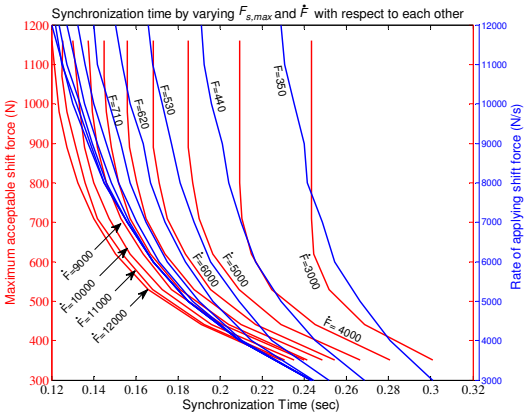

Figure 5: Synchronization time at varying $F_{s,max}$ and $\dot{F}_s$.

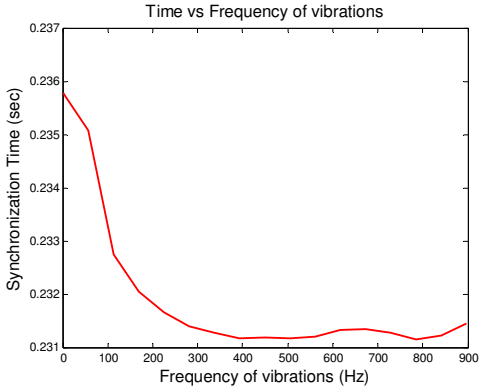

Figure 6: Variation of synchronization time with varying frequency of vibrations.

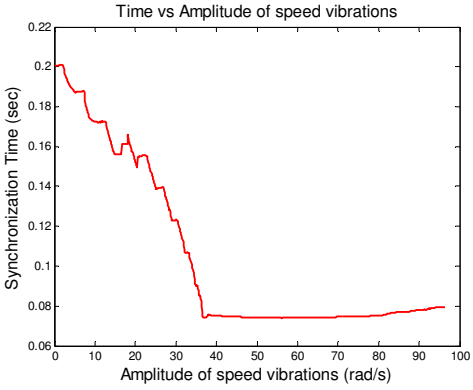

Figure 7 : Variation of synchronization time with varying amplitude of vibrations.

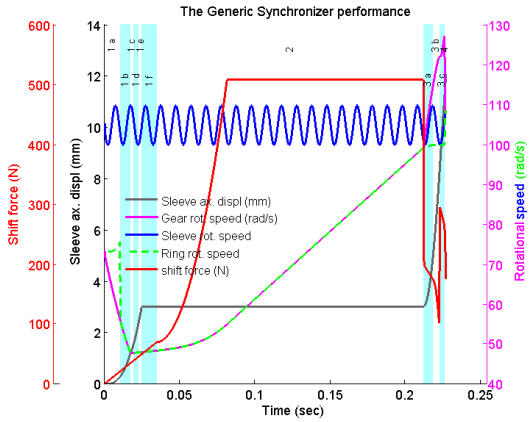

Figure 8: Synchronizer performance diagram with driveline vibrations.

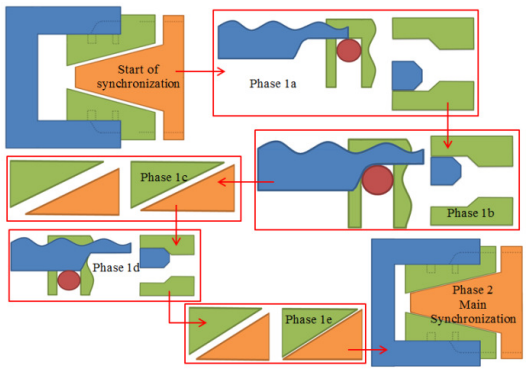

Figure 9: The modified generic synchronizer.

The synchronization time decreases with increasing frequency and amplitude of the vibrations at average values of the phase shift as shown in Figure 6 and 7. Before about 38 rad/s amplitude the decrease in time is sharp with small variations and after not only the time variation is small but also time increases. This kind of behaviour shows that at particular

values of other variables, effects of increase in amplitude upon the synchronization time are limited to a certain value. Figure 8 shows the generic synchronizer performance diagram at 100 Hz frequency of the vibrations and 5 rad/s amplitude of the speed vibrations.

5 MODEL VALIDATION

The generic synchronizer is modified according to the available experimental set-up as shown in Figure 9. Positions of cone and chamfer of the synchronizer ring are exchanged. The sleeve is blocked by the chamfers contact between the sleeve and the ring. The gearwheel and the ring have cones contact. Sub-phase of the spring happen before sub-phase of the viscous friction. Sub-phases of the axial indexing and angular indexing of the ring are also exchange their order. The detailed description is given in [11]. The measured shift force is taken as applied sleeve force in the model and time and speed difference are computed. The performance diagram is shown in Figure 10. From the experimental set-up 9 measurements are taken and the results are agreed closely, see Figure 11.

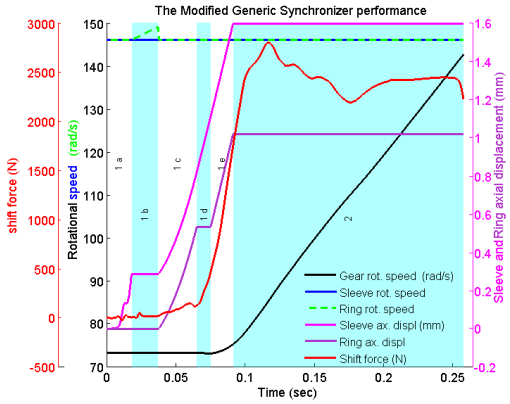

Figure 10: The modified generic synchronization process.

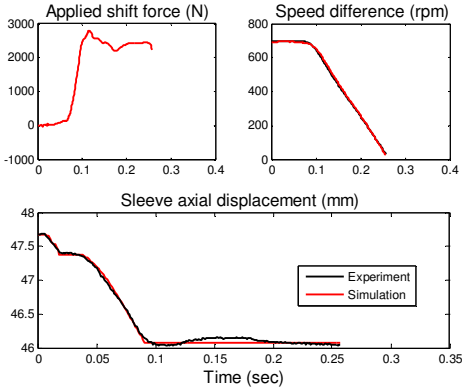

Figure 11: Applied shift force and speed difference during the generic synchronization.

6 CONCLUSIONS AND OUTLOOK

In this paper, the dynamics of a generic synchronizer was modelled using Constrained Lagrangian Formalism with constraints to describe each sub-phase of the synchronization process. The sensitivity analysis for cone angle, coefficient of friction, maximum acceptable shift force and rate of applied shift force and validation against test rig data show that the developed mathematical model using CLF predicts motion and internal forces in the system during the synchronization process reasonably well. Synchronization performance diagram is obtained by also introducing the vibrations to the generic synchronizer. Next, the model will be used to get further insight into synchronizer design with aid of global sensitivity analysis and Pareto optimization.

ACKNOWLEDGMENTS

Scania CV AB, Volvo GTT and the Sweden's Innovation Agency, VINNOVA are gratefully acknowledged for financially supporting the presented research, (project No: 2012-04619). The authors wish to thank Magnus Andersson for suggesting the generic synchronizer and Daniel Häggström and Kenth Hellström for experimental data and fruitful discussions.

REFERENCES

[1] A. Bedmar, *Synchronization processes and synchronizer mechanisms*. Diploma work no. 2013:20 Department of Applied Mechanics, Chalmers University of Technology, Göteborg, Sweden 2013.

[2] L. Lovas, *Etude des relations entre le comportment et la fabrication des synchronisateurs des.* National Institute of Applied Sciences, Lyon, PhD Thesis, 2004.

[3] H. Hoshino, Analysis on Synchronization Mechanism of Transmission. *International Congress and Exposition,* Detroit, Michigan, March 1-4, 1999.

[4] D. Kelly and C. Kent, Gear Shift Quality Improvement In Manual Transmissions Using Dynamic Modelling. *FISITA World Automotive Congress*, Seoul, Korea, June 12-15, 2000.

[5] D. Häggström and M. Nordlander, *Development of a program for calculating gearbox synchronization.* Master thesis, Department of Engineering Sciences and Mathematics, Luleå University of Technology, Luleå, 2011.

[6] P.D. Walker and N. Zhang, Parameter study of synchronizer mechanisms applied to Dual Clutch Transmissions. *Int. J. Powertrains,* vol. 1(2), pp. 198-220, 2011.

[7] A. Sandoza, Double synchronizer to amplify the synchronizer capacity. *SAE technical paper series,* 2012-2003, 2012.

[8] M.K. Sharma and J. Salva, Shift system inertia mass optimization techniques to minimize double bump for manual transmission. *SAE technical paper series,* 2012-01-1999, 2012.

[9] D. Häggström, U. Sellgren and S. Björklund, Robust pre-synchronization in heavy truck transmissions. *In Proc. Of the Int. gear conference*, Lion, 2014.

[10] V. Berbyuk, Towards pareto optimization of performance of a generic synchronizer of transmission systems. In *Proc. of IDETC/CIE ASME 2015*, Boston, USA, 2015 August 2-5, paper DETC 2015-46773.

[11] M. Irfan, V. Berbyuk and H. Johansson, *Constrained Lagrangian Formulation for modelling and analysis of transmission synchronizers.* 2015:05 Department of Applied Mechanics, Chalmers University of Technology, Gothenburg, 2015.

[12] E. J. Haug, *Intermediate Dynamics*, Prentice Hall Englewood Cliffs, New Jersey, 1992.

[13] A. A. Shabana, *Dynamics of multibody system*, Cambridge University Press, Cambridge, 1998 Second edition.